Article

Assessing the Prediction Accuracy of Geomorphon-Based Automated Landform Classification: An Example from the Ionian Coastal Belt of Southern Italy

Dario Gioia [1,*] , **Maria Danese** [1] , **Giuseppe Corrado** [2] , **Paola Di Leo** [3] , **Antonio Minervino Amodio** [1] and **Marcello Schiattarella** [2]

1   National Research Council (CNR), Institute of Heritage Science (ISPC), Tito Scalo, I-85050 Potenza, Italy; maria.danese@cnr.it (M.D.); antonio.minervinoamodio@ispc.cnr.it (A.M.A.)
2   Dipartimento delle Culture Europee e del Mediterraneo (DiCEM), Basilicata University, I-75100 Matera, Italy; giuseppe.corrado@unibas.it (G.C.); marcello.schiattarella@unibas.it (M.S.)
3   National Research Council (CNR), Institute of Methodologies for Environmental Analysis (IMAA), Tito Scalo, I-85050 Potenza, Italy; pdileo@imaa.cnr.it
*   Correspondence: dario.gioial@cnr.it

Abstract: Automatic procedures for landform extraction is a growing research field but extensive quantitative studies of the prediction accuracy of Automatic Landform Classification (ACL) based on a direct comparison with geomorphological maps are rather limited. In this work, we test the accuracy of an algorithm of automatic landform classification on a large sector of the Ionian coast of the southern Italian belt through a quantitative comparison with a detailed geomorphological map. Automatic landform classification was performed by using an algorithm based on the individuation of basic landform classes named geomorphons. Spatial overlay between the main mapped landforms deriving from traditional geomorphological analysis and the automatic landform classification results highlighted a satisfactory percentage of accuracy (higher than 70%) of the geomorphon-based method for the coastal plain area and drainage network. The percentage of accuracy decreased by about 20–30% for marine and fluvial terraces, while the overall accuracy of the ACL map is 69%. Our results suggest that geomorphon-based classification could represent a basic and robust tool to recognize the main geomorphological elements of landscape at a large scale, which can be useful for the advanced steps of geomorphological mapping such as genetic interpretation of landforms and detailed delineation of complex and composite geomorphic elements.

Keywords: automated landform classification; geomorphology; polygenic terraces; Ionian coastal belt; southern Italy

1. Introduction

Automatic Classification of Landform (ACL) is a growing research field and different algorithms and procedures have been incorporated into GIS software with the aim to provide suitable procedures of automatic or unsupervised landform extraction or classification. Most of them simply require a DEM, and the availability of high-resolution DEMs at a global scale has promoted the proliferation of many applications in the fields of geomorphology, geology, archaeology, and urban science [1–6]. Indeed, several works have taken advantage of automated landform classification for the reconstruction of issues related to the complex relationships between the spatial distribution of landforms and landscape evolution [7–9], seismotectonics [10], geoarchaeology [6,11], geodiversity [12], and urban planning [13]. Although such studies have demonstrated the usefulness of automatic procedures of landform extraction, traditional geomorphological analysis cannot be disregarded for the accurate preparation of detailed landform maps. On the other hand, landform maps deriving from algorithms or procedures of unsupervised or semiautomatic

extraction/classification of landforms provide several advantages over the traditional and time-consuming methods of geomorphological mapping (i.e., photointerpretation and field surveys). Firstly, the use of an appropriate algorithm of landform classification overcomes the issue of the subjective interpretation of the "expert" and the low reproducibility of "manual" geomorphological maps. In addition, traditional geomorphological maps usually feature "discrete" landforms but many advanced applications need a full coverage/classification of the study area for the geostatistical analysis of relationships between landform classes and other parameters/factors [14]. Although all these factors should promote the fast growth of the application of ACL methods, the maps derived from such an approach are frequently not able to define fully the spatial pattern of landforms and have a high level of noise. However, a relevant limitation of the method is its high scale-dependence. Landforms pertaining to different geological landscapes have peculiar dimensions and in a first step, the ACL should include the hierarchical definition of type and size of landforms occurring at different scales. Most of the ACL approaches are focused on the characterization of mesoscale landforms (size-scale of hundred meters) and are strictly dependent on the search window size. Finally, this kind of approach does not provide any information about the time and origin of the geomorphic features [1,15], thus implying an additional step of map interpretation.

Due to these limitations, the time-consuming traditional approaches of landform recognition and mapping are still the preferred ones by geomorphologists. On the other hand, few papers provided extensive validation of algorithms and procedures of ACL based on the comparison with "expert"-based geomorphological maps (see for example [1,16,17]). Due to the high potential of ACL, this kind of approach based on the quantitative analysis of the relationships between ACL classes and mapped geomorphological elements can be useful to improve the knowledge of the prediction ability of unsupervised methods of landform classification and should be extensively carried out.

In this paper, we discuss the experimental results of the appliance of an algorithm of automatic landform classification, recently proposed by [18]. Preliminary analysis of the methods of automatic/semiautomatic landform extraction highlights a good potential [2,8,18] but detailed and quantitative studies of its degree of accuracy are lacking. Moreover, the method does not differentiate between gently dipping surfaces and steeper slopes, and it is not able to discriminate the different landforms based on their relative altitudes. Results of the ACL obtained by such an approach have been quantitatively assessed in a test area of the southern Italian coast, where a detailed geomorphological map is available (Figure 1, [19]).
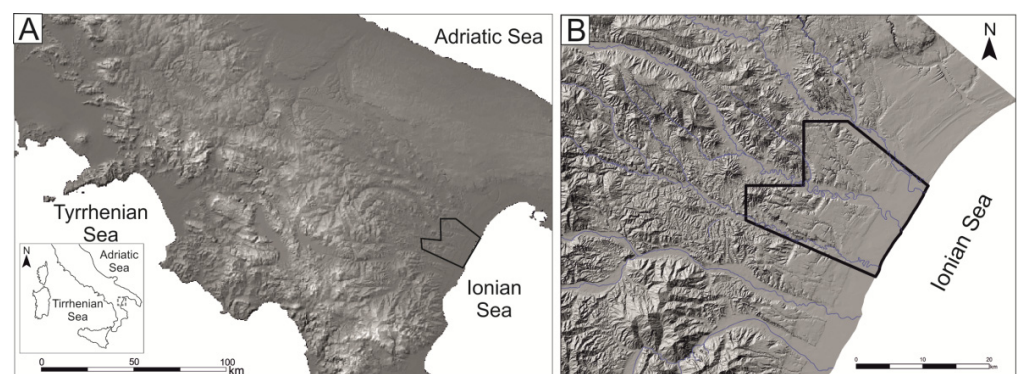

Figure 1. Location of the study area portrayed on a hillshade map of the southern Italy (**A**) and Ionian coastal belt (**B**).

This approach allowed us to evaluate the robustness and reliability of the automatic landform classification and to attribute a geomorphological interpretation to the landforms extracted by unsupervised classification.

2. Materials and Methods

2.1. Study Area: Geological and Geomorphological Framework

The study area is located in the Ionian coastal belt of Basilicata, southern Italy. From a geological viewpoint, it covers a large sector of the foredeep of the southern Apennine chain, not far from the eastern front of the belt. In this sector, a moderate tectonic uplift (<1 mm/year, [20–22]) has occurred since the middle Pleistocene, which led to the progressive emersion of the area and the transition from marine to continental depositional environment. Middle-upper Pleistocene tectonic uplift and eustatic sea-level variations controlled the development of several orders of marine terraces [23,24], which are arranged in a staircase geometry with a regular decrease in altitude from the oldest to the youngest (Figure 2).
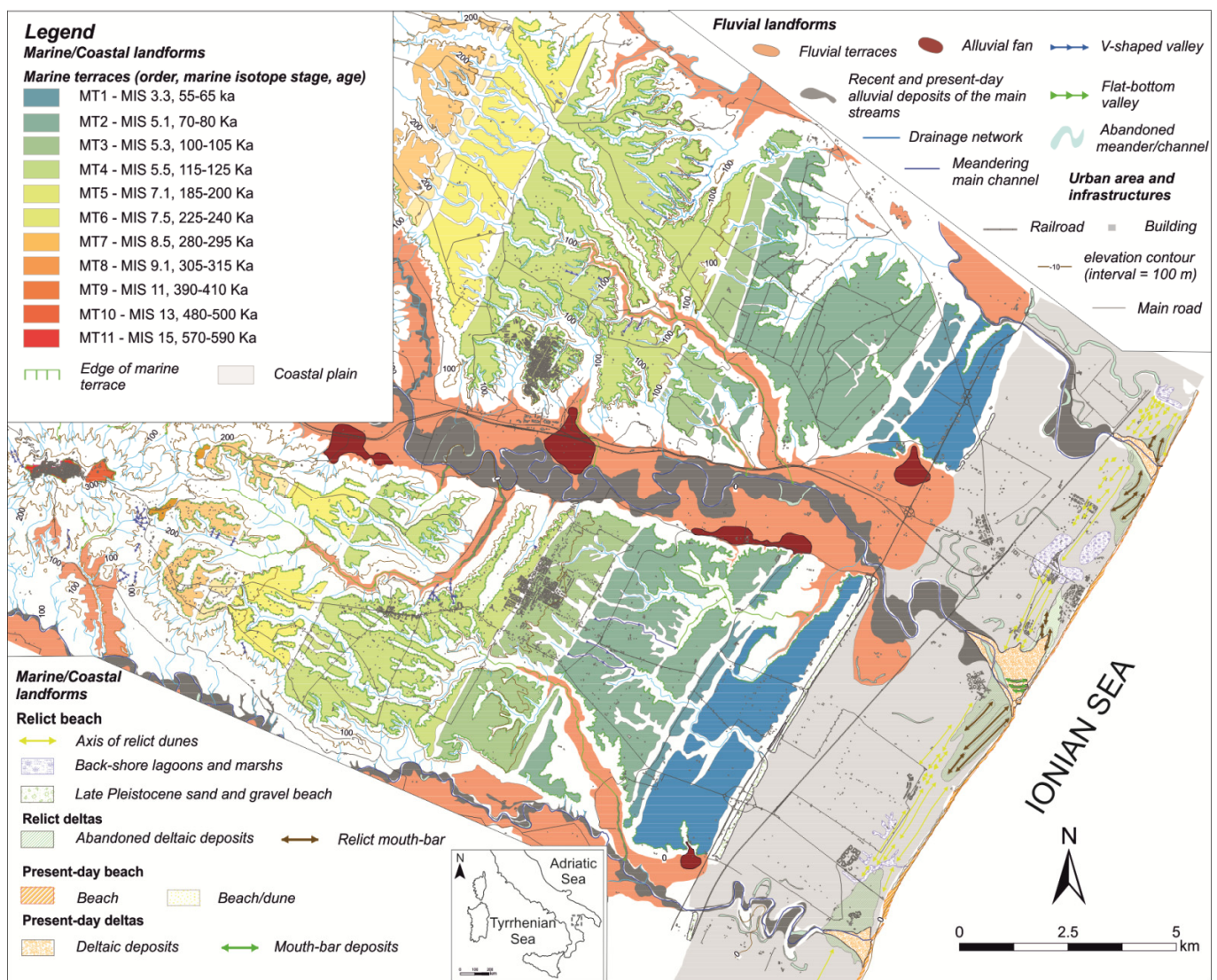
Figure 2. Geomorphological map of the study area (modified by [6,19]).

Marine terraced deposits unconformably overlie a bedrock made by lower Pleistocene marine grey-blue silty clays [6,25]. Marine terrace deposits consist of thin gravel and sand wedges organized in superimposed orders, whereas marine clays largely crop out along the deeper incision of the fluvial net [22]. Marine and transitional deposits are partially covered by younger continental and transitional (marine-continental) deposits, late Quaternary in age.

The alluvial environments are represented by continental deposits, either located along the channels of the main rivers or on wide flood plains, whereas transitional deposits belong to delta and beach environments, whose depositional systems, prograded up to the present-day shoreline during the late Holocene [26].

2.2. Automatic Landform Classification and Comparison with Geomorphological Map

The current methods of ACL are mainly based on the extraction of first and second order DEM-derivative attributes (slope and curvature) and clustering can be cell-based or object-based [9,27]. Local surface shape is frequently combined to the relative slope position of the landform elements to group the landscape sectors with similar statistical parameters and within selected moving windows [28], which strongly control the classification results. Available algorithms are in fact strictly dependent on the moving-windows size and such a limitation can exert a strong influence on the landform scale that the ACL is able to capture.

In this work, we tested the accuracy of an algorithm of automatic landform classification, the geomorphon method [18,29]. It differs from the other existing algorithms of ACL (i.e., the TPI method [4] or Dikau's classification [28]) because it does not use classic map algebra and neighborhood spatial statistic methods to calculate elevation differences inside the search windows. Conversely, it uses a computer vision approach, a pattern-based classification that self-adapts to the local topography. This technique utilizes the line-of-sight principle to evaluate a D quantity in each surrounding; more specifically, the parameter D takes into count not only the elevation differences but also the zenith and nadir angles in the profiles and the lookup distance; thus, the D quantity should ensure the identification of a landform at its most appropriate spatial scale [18].

Landform classification is derived from the extraction of Local Ternary Patterns (LTPs). LTPs are the basic microstructures that constitute each existing type of landform and are named geomorphon; through the combination of geomorphon, landforms are extracted, in particular, the first ten classes given back by the algorithm constitute the most frequent existing landform elements [18]. The algorithm is implemented in the GRASS GIS module named *r.geomorphon* and adopts self-adapting neighborhood statistics with the definition of the following input parameters: DEM, inner and outer search radius, and a flatness threshold. In particular, the outer or maximum search radius (lookup distance) sets the maximum distance for line-of-sight (LOS) calculations for each pixel, which is strictly related to scale recognition of the basic landform class. Automatic extraction was performed using a LIDAR-derived DEM with a spatial resolution of 5 m, which was acquired in 2013 by an airborne LIDAR survey. The DEM is freely available on the geoportal of the Basilicata Regional Authority (http://rsdi.regione.basilicata.it, accessed on 14 October 2021). Input parameters were selected by comparing maps deriving from different input parameters with landforms detected through geomorphological analysis in key sectors of the study area. Such a comparison allowed us to iteratively select the following input parameters: inner radius: 25 m, outer radius: 250 m, and flatness threshold: 2°.

To investigate the relationships between landform classes derived by the automatic extraction and expert-based mapped landforms of the study area, a detailed geomorphological map was prepared in the frame of a wider interdisciplinary EU project (see [5,6,19] for more details) by combining field survey and geomorphological photo-interpretation. The identification and mapping of landforms related to marine, fluvial, and other surface processes were carried out through the photointerpretation of aerial images at a 1:33,000 scale with local field checks on a topographic base map at a 1:10,000 scale. All the recognized landforms were digitized using ArcGIS software to create a final map at a 1:25,000 scale [19]. The map was used as key data to assess the prediction accuracy of the automatic classification.

In order to achieve the evaluation of the automatic landform extraction, the main landforms contained in the traditionally-made map were used. To facilitate the comparison, we transformed linear features in polygons by applying a buffer of 50 m. Then, the overlay

between the two types of maps and the extraction of basic statistics were performed and calculated by using map algebra functions [30,31].

3. Results

3.1. Geomorphological Map

The landscape is characterized by SE-trending gently dipping surfaces of the marine terrace staircase ranging in elevation from 400 m a.s.l. to 10–15 m a.s.l. (Figure 2, [6,19]). The marine terrace staircase is deeply cut by a minor drainage network, which exhibits a trellis-type pattern where marine deposits crop out (i.e., mainly in the westernmost sectors of the study area, see also [22]). In this sector, widespread outcrops of clay deposits are frequently affected by badlands. The investigated area is incised by the lowest reaches of three main rivers, namely, from south to north, the Cavone, Basento, and Bradano rivers. The rivers show a meandering-type thalweg developing on relatively wide alluvial valleys and are morphologically embedded into both Pleistocene marine terraces and clay-rich bedrock. In their lower reaches and in the coastal sectors, the main rivers crosscut the wide flat area of the Metaponto coastal plain and are featured by abandoned channels and large alluvial terraces (Figure 2). Along the flanks of the three valleys, fluvial terraces are distributed in different orders at different elevations.

The flat coastal plain surface represents the top of the sedimentary wedge developed during the Holocene after the last eustatic rise of the sea level that followed the last glacial phase [24]. Until the land reclamation under fascism, the backshore area of the Metaponto coastal plain was characterized by the presence of wide limno-palustrine environments [26]. Landward, the plain leans on the younger late Pleistocene marine terrace of the Metaponto area, reached a maximum elevation of ca. 15 m a.s.l., whereas seaward it ends with the present-day beach. The shore is a low-gradient sandy beach that is limited landward by several-meters-thick sand dunes, striking mainly parallel to the shoreline. Fine marshy deposits have accumulated between these different generations of dunes.

3.2. ACL Map

The results of the automated landform classification of the study area highlight a clear prevalence of the flat areas (Figure 3), which represent about 42% of the study area. Flat classes are distributed along a wide range of altitudes and can be mainly associated to three different landforms: the undissected remnants of the terraced surfaces of (i) fluvial and (ii) marine origin and (iii) the coastal plain (Figure 3). The slope class represents about 14% of the study area and includes the steeper sectors connecting the marine terraces with the lower-altitude alluvial and coastal areas. Other relevant classes of the study area are ridge, shoulder, spur, and valley, which correspond to about 31% of the total area (Figure 3).

Visual comparison between the ACL (Figure 3) and geomorphological maps (Figure 2) highlighted a good correspondence between the main geomorphic elements deriving from the "expert" mapping and geomorphon-based landform classification. In particular, unsupervised classification showed a good accuracy in the delineation of both flat areas of marine and fluvial origin and minor channels of the drainage network. The latter are mainly classified as valley or depression.
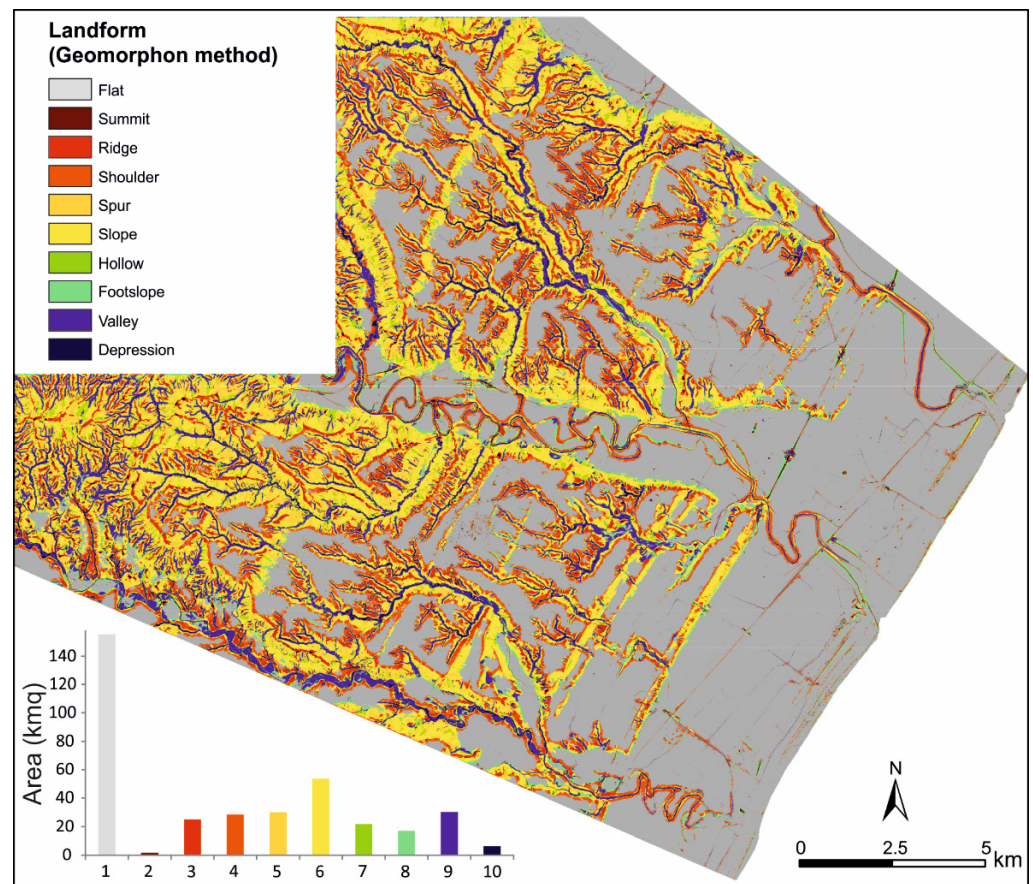
Figure 3. ACL map obtained from the automatic geomorphon method and frequency distribution of the different landform classes.

For a quantitative analysis of the accuracy of landform classes derived by ACL, we estimated the amount of the area and the percentage of the ACL-based landforms for the following mapped elements: marine and fluvial terraces, terrace edges, coastal plain, and channels of the study area. As described above, we converted linear elements of the geomorphological map (i.e., drainage network and terrace edges) into polygons using an appropriate buffer. Results are shown in Figure 4: as expected, the flat class had the highest percentage for low-relief geomorphic elements such as the coastal plain and terraced surfaces (i.e., marine and fluvial terraces). About 91% of the coastal plain was classified as flat areas, whereas other relevant classes of the ACL in the coastal plain were footslope (3.1% of the total area), shoulder, (2.7%), ridge (0.9%), and valley (0.7%). Such landforms represent small-scale landforms of the plain such as relict dune ridges, abandoned meanders, and depressed back-dune areas (see comparison of the maps in Figure 2). More specifically, dune ridges were mainly classified as ridge or shoulder whereas abandoned meanders and backridges were mainly assigned to valley and footslope, respectively.
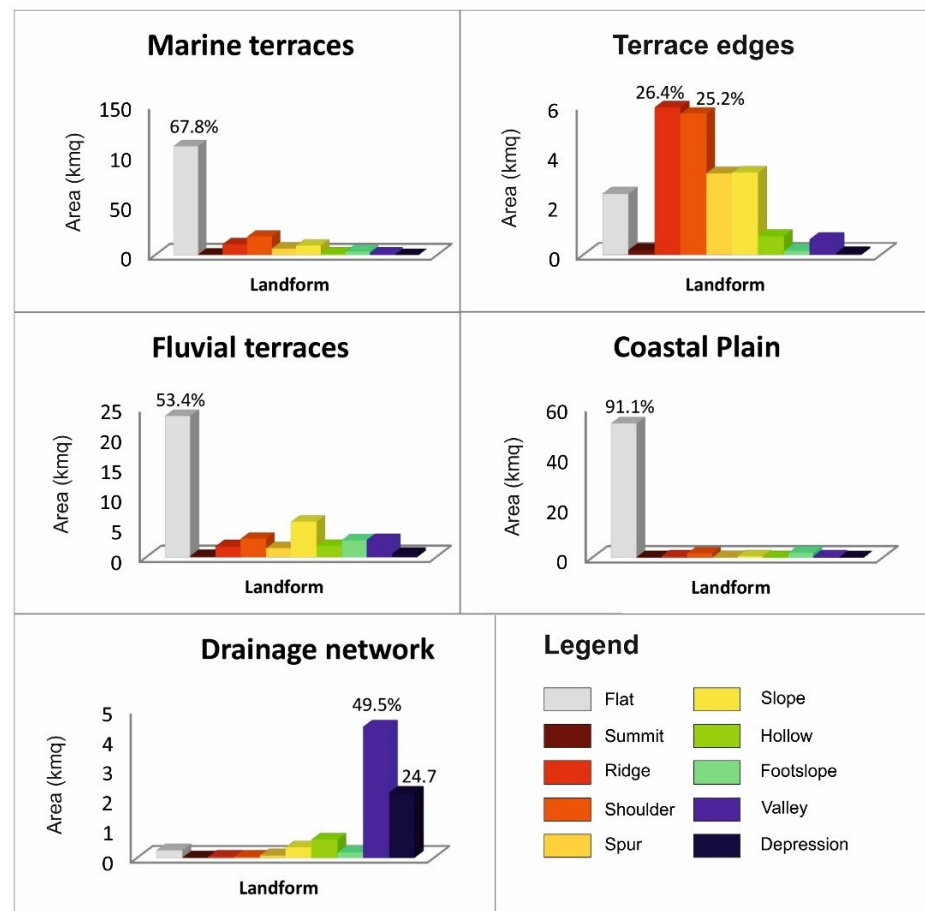
Figure 4. Histograms of automatic extracted landforms contained by each mapped landform (marine terrace, terrace edge, fluvial terrace, coastal plain, and drainage network). In each histogram, the percentage of the predominant class inside the evaluated landform is reported.

The percentage of flat areas for marine and fluvial terraces was slightly lower than the coastal plain (Figure 4), but the automatic extraction showed again a good degree of delineation of the terraced surfaces. Low-angle central and undissected sectors of the marine terraces were well delineated, especially for the lower-altitude orders (see for example Figure 5b). On the contrary, higher-altitude and older orders of marine terraces were affected by widespread fluvial and slope erosion processes and are reduced to small and gently dipping remnants (see for example Figure 5b). Due to this peculiar feature, the areal extent of flat areas was strongly reduced for higher-altitude marine terraces and small remnants of the highest orders were mainly attributed to the "Summit" or "Ridge" classes.

Terrace edges are another peculiar geomorphic element of the study area, which appeared to be captured by geomorphon-based classification: they were mainly classified as "ridge" and "shoulder" (Figure 4) with about 50% of the total area of (Figure 3). For this landform, a significant percentage of pixels (i.e., 40% of the total area) of the ACL map fell into "slope", "spur", and "flat" classes, thus suggesting a lower degree of accuracy of the automatic classification in delineating the sectors joining the higher-altitude landforms and the steeper slopes. On the contrary, steeper slopes and V-shaped valleys were the landform groups that the automatic classification returned well. In particular, a significant value of 75% of the total area was observed for the overlay between the "expert" delineation of the drainage network and related geomorphon-based classes (i.e., valley and depression).
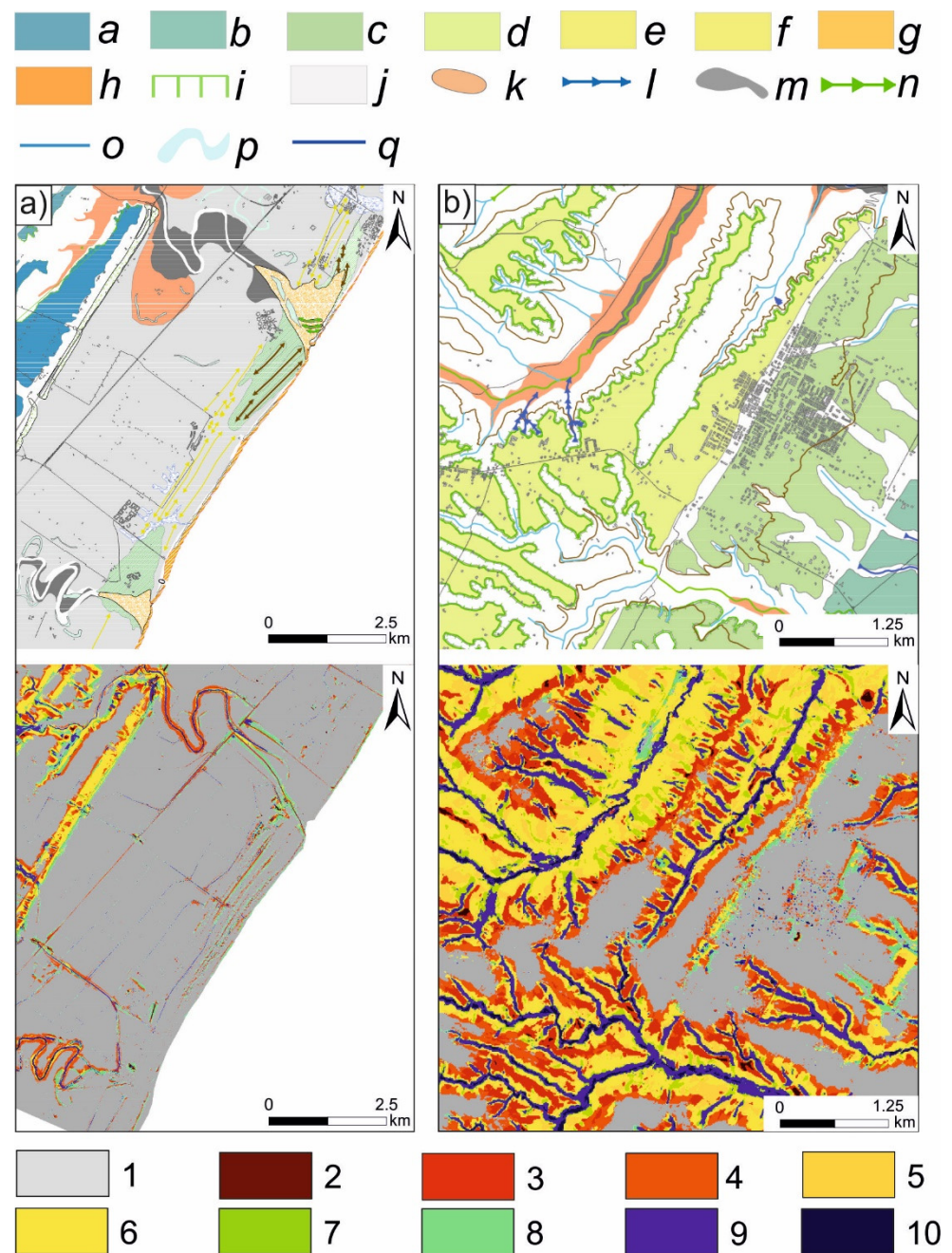
Figure 5. Detail of the comparison between "manual" and automatic landform maps in selected areas of the test site. Geomorphological map: (a) MT1; (b) MT2; (c) MT3; (d) MT4; (e) MT5; (f) MT6; (g) MT7; (h) MT8; (i) Edge of marine terrace; (j) Coastal plain; (k) Fluvial Terraces; (l) V-shaped valley; (m) Recent and present-day alluvial deposits of the main streams; (n) Flat-bottom valley; (o) Drainage network; (p) Abandoned meander/channel; and (q) Meandering main channel. Geomorphon-based map: (1) Flat; (2) Summit; (3) Ridge; (4) Shoulder; (5) Spur; (6) Slope; (7) Hollow; (8) Footslope; (9) Valley; and (10) Depression.

4. Discussion and Concluding Remarks

Many advanced geostatistical approaches of automatic landform classification such as multivariate statistics [4,28], fuzzy logic and unsupervised classification [32], object-oriented image classification [27], and neural networks [33] have been developed to extract object-based or pixel-based landform classes at different scales and spatial resolution.

Although the results of automatic classification are generally considered satisfactory, extensive quantitative studies of prediction accuracy of ACL based on a direct comparison with geomorphological maps are rather limited. Moreover, several works highlight that an increase in both procedure and input data complexities and the number of landform classes does not result in a general improvement of the automatic classification. In particular, most of ACL maps consist of a limited number of classes (i.e., generally 10–12 classes, see for example [1,2,11]), which delineate only the principal geomorphic elements of a landscape. This limitation can be significant in complex and fragmented landscapes. For example, the geomorphological map of our study area was simplified by excluding smaller-scale features, such as landslides and badlands, but includes about 20 geomorphic elements, such as fluvial, slope, marine, and coastal landforms. The ACL map derived by the geomorphon-based algorithm is a fast and easy-to-use approach, although results are clearly less detailed than the "manual" map. The ACL map shows only the principal landform features of the landscapes and does not differentiate among landforms with a similar topographic feature but different origin.

In order to estimate the degree of accuracy of the automatic method of landform classification, we statistically evaluated the spatial overlay between the main mapped landforms and the ACL results. The basic assumption of such an estimation is that the "correct" classification of mapped landforms coincides with higher classes of the ACL map (e.g., we assumed that a "correct" automatic classification of coastal plain was the flat class of ACL map, which corresponded to the dark blue color in the map). Results are shown in Figure 6; a higher percentage of accuracy was observed from the coastal plain area, which was classified as flat with about 91%, whereas the percentage of accuracy decreased by about 20–30% for marine and fluvial terraces.

The overlay between the mapped drainage network and valley and depression classes was about 74%, suggesting a good degree of accuracy of the method in the delineation of the drainage network of the study area. Terrace edges were prevalently classified as ridge and shoulder, and these two classes covered about 51.6% of the manually-drawn terrace edge landforms. The overall accuracy of the ACL map was 69%, which can be considered satisfactory as a preliminary delimitation of widespread geomorphological elements of large areas such as flat plain, terraced surfaces, and drainage network features.

Our results suggest that geomorphon-based classification could represent a basic and robust tool to recognize the main geomorphological elements of landscape at a large scale, which can be useful for next and advanced steps of geomorphological mapping such as genetic interpretation of landforms and detailed delineation of complex and composite geomorphic elements. Such a refining of the automatic classification could be performed using more complex segmentation processes on different scales or including other landscape metrics in the classification procedure such as altitude, relative topographic position, or landscape roughness.
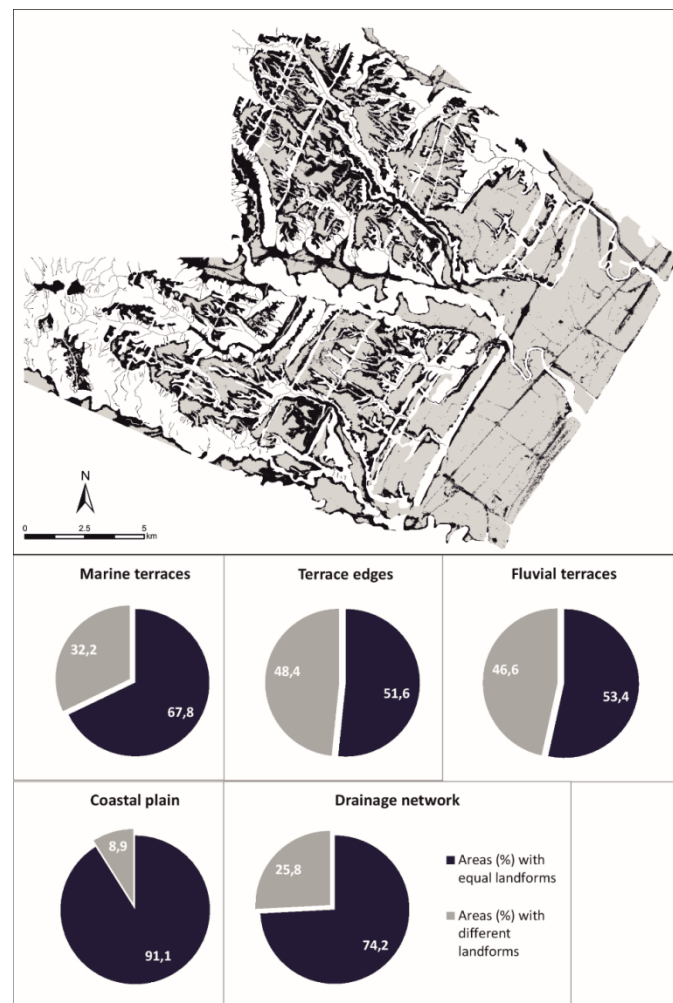
Figure 6. Visual and quantitative comparison between areas with equal (in grey) and different (in dark blue) landforms obtained from the comparison between the automatic and the expert-based map. In the diagrams it is possible to read the percentage of similarity/dissimilarity for each landform, which has been extracted by the spatial overlay between mapped landforms (i.e., marine terraces, terrace edges, fluvial terraces, coastal plain, and drainage network) and prevalent classes of the geomorphon-based map (see text for additional details).

Conflicts of Interest: The authors declare no conflict of interest.

References

1. Wieczorek, M.; Migoń, P. Automatic relief classification versus expert and field based landform classification for the medium-altitude mountain range, the Sudetes, SW Poland. *Geomorphology* **2014**, *206*, 133–146. [CrossRef]
2. Kramm, T.; Hoffmeister, D.; Curdt, C.; Maleki, S.; Khormali, F.; Kehl, M. Accuracy Assessment of Landform Classification Approaches on Different Spatial Scales for the Iranian Loess Plateau. *ISPRS Int. J. Geo-Inf.* **2017**, *6*, 366. [CrossRef]
3. Caruso, A.S.; Clarke, K.D.; Tiddy, C.J.; Delean, S.; Lewis, M.M. Objective Regolith-Landform Mapping in a Regolith Dominated Terrain to Inform Mineral Exploration. *Geosciences* **2018**, *8*, 318. [CrossRef]
4. De Reu, J.; Bourgeois, J.; Bats, M.; Zwertvaegher, A.; Gelorini, V.; De Smedt, P.; Chu, W.; Antrop, M.; De Maeyer, P.; Finke, P.; et al. Application of the topographic position index to heterogeneous landscapes. *Geomorphology* **2013**, *186*, 39–49. [CrossRef]
5. Di Leo, P.; Bavusi, M.; Corrado, G.; Danese, M.; Giammatteo, T.; Gioia, D.; Schiattarella, M. Ancient settlement dynamics and predictive archaeological models for the Metapontum coastal area in Basilicata, southern Italy: From geomorphological survey to spatial analysis. *J. Coast. Conserv.* **2018**, *22*, 865–877. [CrossRef]
6. Gioia, D.; Bavusi, M.; Di Leo, P.; Giammatteo, T.; Schiattarella, M. A Geoarchaeological Study of the Metaponto Coastal Belt, Southern Italy, Based on Geomorphological Mapping and Gis-Supported Classification of Landforms. *Geogr. Fis. E Din. Quat.* **2016**, *39*, 137–147.
7. Xiong, L.-Y.; Zhu, A.-X.; Zhang, L.; Tang, G.-A. Drainage basin object-based method for regional-scale landform classification: A case study of loess area in China. *Phys. Geogr.* **2018**, *39*, 523–541. [CrossRef]
8. Gioia, D.; Danese, M.; Bentivenga, M.; Pescatore, E.; Siervo, V.; Giano, S.I. Comparison of Different Methods of Automated Landform Classification at the Drainage Basin Scale: Examples from the Southern Italy. In *Computational Science and Its Applications—ICCSA 2020*; Lecture Notes in Computer Science; Springer: Cham, Switzerland, 2020; pp. 696–708.
9. D'Oleire-Oltmanns, S.; Eisank, C.; Dragut, L.; Blaschke, T. An Object-Based Workflow to Extract Landforms at Multiple Scales From Two Distinct Data Types. *IEEE Geosci. Remote Sens. Lett.* **2013**, *10*, 947–951. [CrossRef]
10. Wei, Z.; He, H.; Hao, H.; Gao, W. Automated mapping of landforms through the application of supervised classification to lidar-derived dems and the identification of earthquake ruptures. *Int. J. Remote Sens.* **2017**, *38*, 7196–7219. [CrossRef]
11. Verhagen, P.; Dragut, L. Object-based landform delineation and classification from DEMs for archaeological predictive mapping. *J. Archaeol. Sci.* **2012**, *39*, 698–703. [CrossRef]
12. Danese, M.; Gioia, D.; Amodio, A.M.; Corrado, G.; Schiattarella, M. A Spatial Method for the Geodiversity Fragmentation Assessment of Basilicata Region, Southern Italy. In *Computational Science and Its Applications—ICCSA 2021*; Lecture Notes in Computer Science; Springer: Cham, Switzerland, 2021; pp. 620–631.
13. Manfré, L.A.; de Nóbrega, R.A.; Quintanilha, J.A. Regional and local topography subdivision and landform mapping using SRTM-derived data: A case study in southeastern Brazil. *Environ. Earth Sci.* **2015**, *73*, 6457–6475. [CrossRef]
14. Danese, M.; Gioia, D.; Biscione, M.; Masini, N. Spatial methods for archaeological flood risk: The case study of the neolithic sites in the Apulia region (southern Italy). In *International Conference on Computational Science and Its Applications—ICCSA 2014*; Springer: Berlin/Heidelberg, Germany, 2014; pp. 423–439.
15. Dramis, F.; Guida, D.; Cestari, A. Chapter Three—Nature and Aims of Geomorphological Mapping. In *Developments in Earth Surface Processes*; Smith, M.J., Paron, P., Griffiths, J.S., Eds.; Elsevier: Amsterdam, The Netherlands, 2011; pp. 39–73.
16. Teofilo, G.; Gioia, D.; Spalluto, L. Integrated geomorphological and geospatial analysis for mapping fluvial landforms in Murge basse karst of Apulia (Southern Italy). *Geosciences* **2019**, *9*, 418. [CrossRef]
17. Klingseisen, B.; Metternicht, G.; Paulus, G. Geomorphometric landscape analysis using a semi-automated GIS-approach. *Environ. Model. Softw.* **2008**, *23*, 109–121. [CrossRef]
18. Jasiewicz, J.; Stepinski, T.F. Geomorphons—A pattern recognition approach to classification and mapping of landforms. *Geomorphology* **2013**, *182*, 147–156. [CrossRef]
19. Gioia, D.; Bavusi, M.; di Leo, P.; Giammatteo, T.; Schiattarella, M. Geoarchaeology and geomorphology of the Metaponto area, Ionian coastal belt, Italy. *J. Maps* **2020**, *16*, 117–125. [CrossRef]
20. Caputo, R.; Salviulo, L.; Bianca, M. Late Quaternary activity of the Scorciabuoi Fault (southern Italy) as inferred from morphotectonic investigations and numerical modeling. *Tectonics* **2008**, *27*, TC3004. [CrossRef]
21. Westaway, R.; Bridgland, D. Late Cenozoic uplift of southern Italy deduced from fluvial and marine sediments: Coupling between surface processes and lower-crustal flow. *Quat. Int.* **2007**, *175*, 86–124. [CrossRef]
22. Gioia, D.; Schiattarella, M.; Giano, S. Right-Angle Pattern of Minor Fluvial Networks from the Ionian Terraced Belt, Southern Italy: Passive Structural Control or Foreland Bending? *Geosciences* **2018**, *8*, 331. [CrossRef]
23. Cilumbriello, A.; Sabato, L.; Tropeano, M.; Gallicchio, S.; Grippa, A.; Maiorano, P.; Mateu-Vicens, G.; Rossi, C.A.; Spilotro, G.; Calcagnile, L.; et al. Sedimentology, stratigraphic architecture and preliminary hydrostratigraphy of the Metaponto coastal-plain subsurface (Southern Italy). *Mem. Descr. Carta Geol. D'italia* **2010**, *90*, 67–84.
24. Tropeano, M.; Cilumbriello, A.; Sabato, L.; Gallicchio, S.; Grippa, A.; Longhitano, S.G.; Bianca, M.; Gallipoli, M.; Mucciarelli, M.; Spilotro, G. Surface and subsurface of the Metaponto Coastal Plain (Gulf of Taranto-southern Italy): Present-day- vs. LGM-landscape. *Geomorphology* **2013**, *203*, 115–131. [CrossRef]

25. Tropeano, M.; Sabato, L.; Pieri, P. Filling and cannibalization of a foredeep: The Bradanic Trough, Southern Italy. *Sediment Flux Basins Causes Control. Conseq.* **2002**, *191*, 55–79. [CrossRef]
26. Pescatore, T.; Pieri, P.; Sabato, L.; Senatore, M.R.; Gallicchio, S.; Boscaino, M.; Cilumbriello, A.; Quarantiello, M.; Capretto, G. Stratigrafia dei depositi pleistocenico-olocenici dell'area costiera di Metaponto compresa fra Marina di Ginosa ed il Torrente Cavone (Italia meridionale): Carta geologica in scala 1:25.000. *Il Quat. Ital. J. Quat. Sci.* **2009**, *22*, 307–324.
27. Drăguţ, L.; Blaschke, T. Automated classification of landform elements using object-based image analysis. *Geomorphology* **2006**, *81*, 330–344. [CrossRef]
28. Dikau, R.; Brabb, E.E.; Mark, R.K.; Pike, R.J. Morphometric landform analysis of New Mexico. *Z. Geomorphol. Suppl.* **1995**, *101*, 109–126.
29. Hengl, T.; Reuter, H.I. Geomorphometry: Concepts, Software, Applications. In *Developments in Soil Science*; Elsevier: Amsterdam, The Netherlands, 2008.
30. Tomlin, C.D. *GIS and Cartographic Modeling*; Esri Press: Hong Kong, China, 2013.
31. DeMers, M.N. *Fundamentals of Geographic Information Systems*; Wiley: Hoboken, NJ, USA, 2008.
32. Burrough, P.A.; van Gaans, P.F.M.; MacMillan, R.A. High-resolution landform classification using fuzzy k-means. *Fuzzy Sets Syst.* **2000**, *113*, 37–52. [CrossRef]
33. Ehsani, A.H.; Quiel, F. Geomorphometric feature analysis using morphometric parameterization and artificial neural networks. *Geomorphology* **2008**, *99*, 1–12. [CrossRef]